Size Effects and Passivation Effects on the Plasticity of Freestanding Submicron Gold Films

H. D. Espinosa and B. C. Prorok
Department of Mechanical Engineering, Northwestern University
2145 Sheridan Road, Evanston, IL 60208-3111, USA

ABSTRACT
The Membrane Deflection Experiment was used to examine size effects on freestanding thin film gold membranes. It is the first micro-scale testing scheme where the loading procedure is straightforward and accomplished in a highly sensitive manner while preserving the independent measurement of stress and strain. Stress-strain curves were obtained on films 0.3, 0.5 and 1.0 µm thick including membrane widths of 2.5, 5.0, 10.0 and 20.0 µm for each thickness. Both membrane thickness and width were shown to cause size effects on the mechanical properties. By far, thickness played a major role in deformation behavior exhibiting a major transition in the material inelastic response occuring when thickness was changed from 1.0 to 0.5 µm. In this transition, the yield stress more than doubled when film thickness was decreased, with the 0.5 µm thick specimen exhibiting a more brittle-like failure and the 1.0 µm thick specimen exhibiting a strain softening behavior. Results of the effect of surface passivation, with 30 nm SiO_2 layers, showed a decrease in yield stress with passivation opposite to that reported in other studies.

INTRODUCTION
Most knowledge of material properties exists at the bulk-scale regime where known constitutive laws material describe behavior. When specimen size becomes small, in the micron regime, these laws fail to describe material response. Thin films, which are commonly employed in microelectronic components and MEMS devices, often display mechanical behavior that cannot be described by traditional means. Their mechanical properties are often essential to the device function and therefore accurate identification is key in determining the device reliability.

The affect of specimen size on material mechanical behavior has been experimentally studied by several researchers. Results on nanoindentation [1-5], torsion of microscale rods [6], and bending of thin films [7] have all shown that as specimen size decreased to the micron regime the strength of the film increased. However, in these studies each method subjects the specimens to large strain gradients. Modified plasticity theories have incorporated these strain gradients into a continuum description of microscale deformation behavior [6,8-11].

In this work the Membrane Deflection Experiment (MDE) is used to test the mechanical response of sub-micron gold films [12-15]. The MDE test has certain advantages for the microscale mechanical testing of thin films. The simplicity of sample microfabrication and ease of handling lend confidence in repeatability. The loading procedure is straightforward and accomplished in a highly sensitive manner while preserving the independent measurement of stress and strain. The measurements are also performed under macroscopic homogeneous axial deformation, i.e., in the absence of deformation gradients, in contrast to nanoindentation, torsion, and bending of thin films where deformation gradients naturally occur. We will also evaluate the effect of 30 nm thick SiO_2 passivation layers on plasticity and fracture of thin gold film.

EXPERIMENTAL PROCEDURE
Specially designed thin film Au specimens were microfabricated on (100) Si wafers. Specimen shape was defined on the topside by photolithography and lift off with selective etching of bottom side windows with the purpose of creating suspend membranes, see Espinosa et al. [13] for further details. Passivation layers were grown on both sides of the gold membrane through plasma assisted CVD.

The geometry of the suspended thin-film membranes can be described best as a double dog-bone tensile specimen. Fig. 1(a) shows an optical image of the Au membranes. Membrane width was varied in each die, to examine size effects, while preserving the ratio of gauge-length/width. Dimensions of four differently sized membranes can be described by their widths, W, of 2.5, 5, 10 and 20 um.

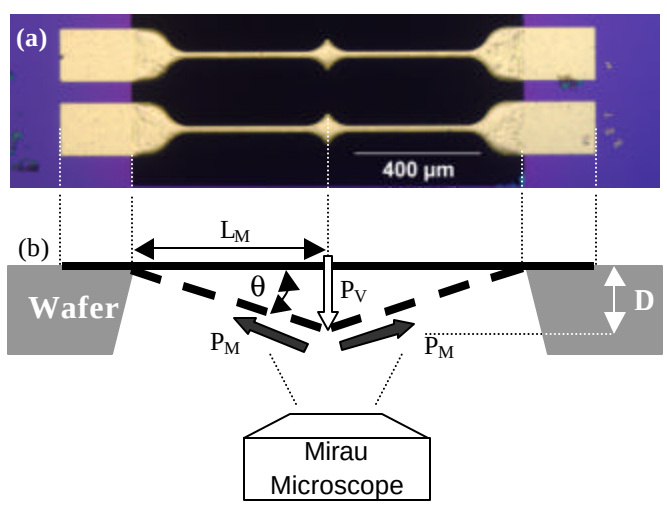

Fig. 1. (a) An optical image showing the topside of the Au membranes and (b) a side view of the MDE test. Parameters are defined in the text.

The Membrane Deflection Experiment (MDE) was used to achieve direct tensile stressing of the specimens [12,13]. The procedure involves applying a line-load, with a nanoindenter, at the center of the spanning membrane. Simultaneously, an interferometer focused on the bottom side of the membrane records the deflection. The result is direct tension in the gauged regions of the membrane with load and deflection being measured independently.

The data directly obtained from the MDE test must then be reduced to arrive at a stress-strain signature for the membrane. The load in the plane of the membrane is found as a component of the vertical nanoindenter load by the following equation:

$$\tan\theta = \frac{\Delta}{L_M} \quad \text{and} \quad P_M = \frac{P_V}{2\sin\theta}, \tag{1}$$

where (from Fig. 1b) θ is the angle of rotation, Δ is the displacement, L_M is the membrane half-length, P_M is the load in the plane of the membrane, and P_V is the load measured by the nanoindenter. Once P_M is obtained the Cauchy stress, $\sigma(t)$, can be computed from:

$$\sigma(t) = \frac{P_M}{A}, \tag{2}$$

where A is the cross-sectional area of the membrane in the gauge region. The cross-sectional area dimensions were measured using an Atomic Force Microscope (AFM).

The interferometer yields vertical displacement information in the form of monochromatic images taken at periodic intervals. The relationship for the distance between interference fringes, δ, is related through the wavelength, λ, of the monochromatic light used. By finding the average distance between the number of fringes that are in the focal plane of the interferometer, an overall strain, $\varepsilon(t)$, for the membrane can be computed from the following relation [13],

$$\varepsilon(t) = \frac{\sqrt{\delta^2 + (\lambda/2)^2}}{\delta} - 1, \tag{3}$$

RESULTS AND DISCUSSION

Fig. 2 shows a scanning electron microscopy image for a membrane 0.5 µm thick, see Espinosa and Prorok [14] for images of 0.3 and 1.0 µm thick specimens. Note that a 45° tilt was employed in the image to better examine the specimen width, thus the dimensions of the membrane are skewed with respect to the micron bar. The microstructure consists of equiaxed grains with an average size of 250-300 nm. The membranes have a characteristic number of grains through their thickness. The 0.3 µm thick membrane has approximately 2 grains, the 0.5 µm thick membrane 2-3 grains, and the 1.0 µm thick membrane 4-5 grains through the thickness. Likewise, the membranes of different width also have a variable number of grains traversing the membrane width. They range from 8-10 for a width of 2.5 µm to 66-80 for a width of 20 µm. These characteristics will likely have an effect on the mechanical response of the membranes in the context of statistical distributions of dislocation sources, grain boundary types, and slip systems.

Another aspect of the microstructure to consider is texture. Fig. 3 is the result of micro-diffraction normal to the membrane surface. It indicates a strong <111> texture exists normal to the film surface. Thus, the modulus of the films in the plane of the membranes will likely be in the range of the <100> and <110> crystallographic direction. For instance, the moduli of gold in different directions are $E_{<111>}$ = 117 GPa, and $E_{<100>}$ = 43 GPa [16].

Figs 4 shows the stress strain plots obtained from the membrane deflection experiments. This plot compares the effect of membrane thickness for the 5.0 µm width membrane. See Espinosa and Prorok [14] for stress-strain curves for widths of 2.5, 10.0 and 20.0 µm. All three curves possess a Young's modulus of 54 GPa, dashed line in Fig. 4. The curves for membranes of thickness 0.3 and 0.5 µm show nearly identical elastic and plastic behavior, σ_y=170 MPa, with the exception that the 0.5 µm thick membrane exhibits a larger failure strain. The curves match each other so well that it is difficult to discern where the 0.3 µm thick specimen fails. This is signified by the arrow at ε=0.0075. Contrasting deformation behavior is exhibited by the 1.0 µm

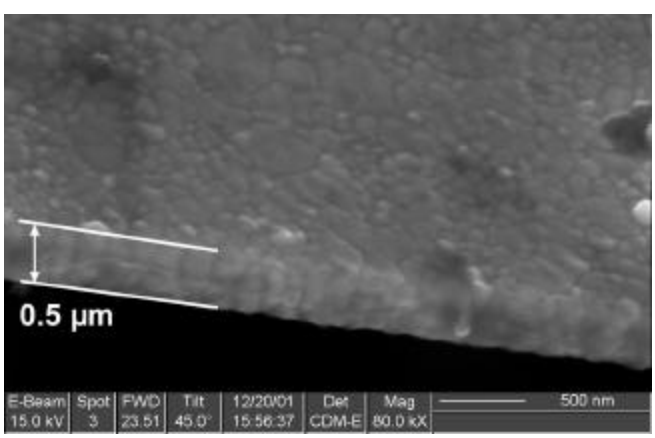

Fig. 2. SEM image highlighting the number of grains existing through the film thickness. Note 45° tilt of SEM stage.

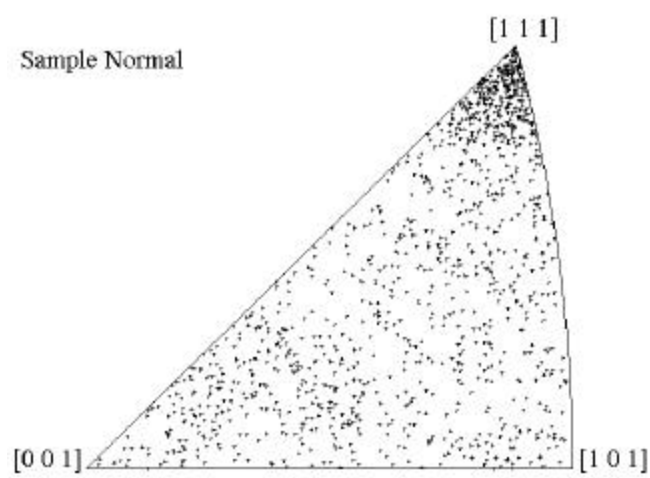

Fig. 3. Pole figure showing the strong <111> texture normal to the film surface.

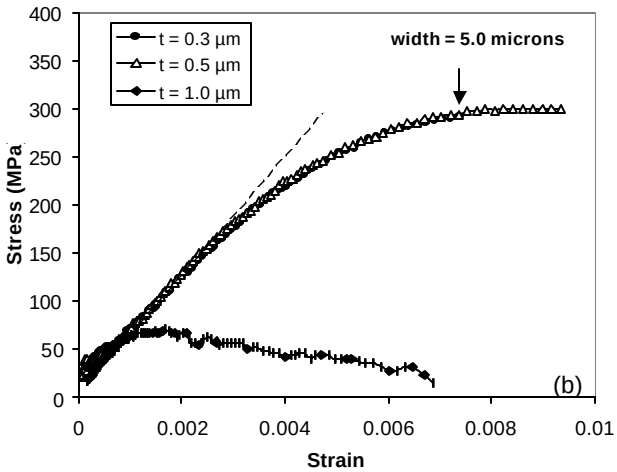

Fig. 4. Stress-Strain plot for membranes 5.0 µm wide and 0.3, 0.5 and 1.0 µm thick. Arrow signifies failure point of the 0.3 µm thick membrane.

thick membrane. Yield stress decreased considerably to 65 MPa and plastic deformation occurred mostly in discrete quantities with an overall continual decrease in stress to failure. In comparing the grain morphology through the thickness of the films it can be seen that the 1.0 µm thick film contains 4-5 grains whereas the thinner films contain considerably less. This is an indication there is a higher propensity for intergranular deformation processes to occur in the thicker film.

Identical behavior is exhibited for the other membrane widths of 2.5, 10.0 and 20.0 µm [14]. In all of the different specimens tested, yield stress best denotes the effect of size on behavior. Table 1 summarizes these values. From this table, it is clear that both thickness and width effects are present. In terms of thickness, a major increase in the onset of anelastic behavior occurs when thickness is decreased below 1.0 µm. This is a clear indication that the membranes are strengthened as a result of thickness reduction. As previously mentioned, this effect is realized by the microstructure morphology through the film thickness.

When considering the effect of width, the number of grains across the width must be examined. For the 2.5 µm wide membrane an average of 8-10 grains traverse the width, 16-20 for 5.0 µm, 32-40 for 10.0 µm, and 66-80 for a width of 20 µm. It is clear that the number of grains contained in the width and the variation of yield strength with width shown in Table 1 also affect the onset of plastic yielding. The trend appears to be, the more grains, the lower the yield stress. This could result from strong statistical effects due to the small number of grains.

Table 1. Values of yield stress (σ_y) in MPa for all specimens.

	Width			
Thickness	**2.5 µm**	**5.0 µm**	**10.0 µm**	**20.0 µm**
0.3 µm	220	170	170	170
0.5 µm	220	170	170	140
1.0 µm	90	65	55	55

It is clear that such small numbers of grains restrict dislocation motion. Because so few grains span the thickness and width, the sources of plastic deformation are reduced resulting in increased yield strengths.

Fig. 5 is a scanning electron microscopy image of the failure region for a membrane with a thickness of 1.0 µm. Multiple striations or deformation bands are seen near the failure region. They run in a direction perpendicular to the tensile load. These are regions where discrete permanent deformation has occurred and may be related to the jogs seen in the stress-strain curve of Fig 4. Bands of this sort are seen in bulk materials during the development of texture with deformation [17]. Along the fracture surface the gold appears to have undergone large localized plastic deformation with ductile like fingers in the stretching direction. The formation of multiple bands is a clear indication that the membrane was uniformly loaded.

Contrasting fracture behavior was exhibited for membranes 0.3 and 0.5 um thick. These membranes fractures in a brittle-like manner, see Fig 6. This image is illustrative of the change in deformation behavior observed in the stress-strain analysis as thickness was reduced from 1.0 to 0.5 µm. No deformation bands were observed for membranes of this thickness or thinner. Although some ductility occurred, evidenced by ductile-like fingers on the fracture surface. These findings are consistent with the measured stress-strain curves.

The effect of passivation layers on yielding behavior of the gold films was also examined. This was accomplished by depositing 30 nm layers of SiO_2 on either side of the 0.5 µm thick membranes. MDE results from these specimens can then be compared with the previous results of this study. Fig. 8 shows stress-strain curves comparing the passivated and unpassivated membranes 0.5 um thick and 5.0 µm wide. In order to directly compare the two signatures, compatibility issues must be considered in the passivated membranes. In comparing the two signatures, we assumed compatibility of deformation exists until membrane fracture for the passivated films. That is, both films, Au and SiO_2, remain intact and perfectly bonded with each carrying a portion of the applied load.

In comparing the stress-strain signatures for the 5.0 µm width, Fig 8, several aspects are apparent. First, both the passivated (□) and unpassivated (◆) membranes have nearly identical Young's modulus, ≅ 54 GPa. Also, It is clear from extrapolation to zero strain of the elastic regions, see plot inset, that the passivated film has a residual stress of approximately 45 MPa while the unpassivated film has a residual stress of about 33 MPa. Yield stress also varies widely from 133 to 170 MPa for the passivated and unpassivated membranes, respectively. Failure of the

Table 2. Values of σ_y and σ_r with and without passivation.

Width ➲		**2.5 µm**	**5.0 µm**	**10.0 µm**	**20.0 µm**
Unpassivated	σ_y	220	170	170	170
	σ_r	35	33	23	21
Passivated	σ_y	125	133	140	52
	σ_r	55	45	30	28

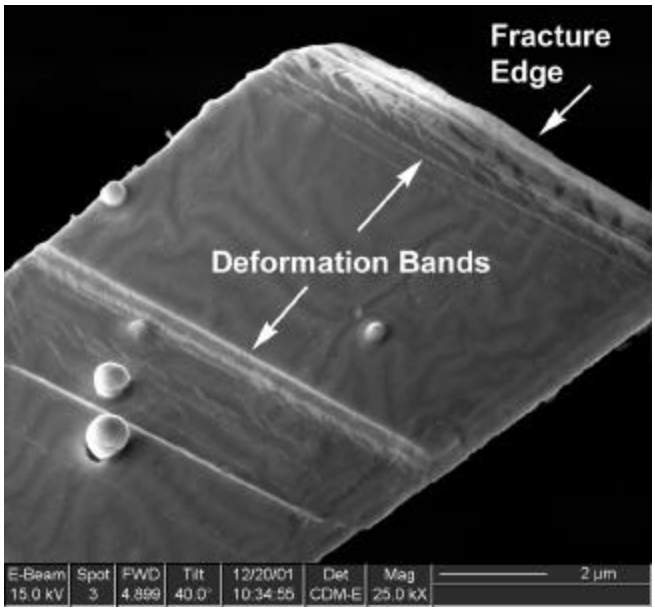

Fig. 6. SEM image of a fracture for a film thickness of 1.0 µm. The symbol "n" denotes nodules of gold that exist as an element of the film structure.

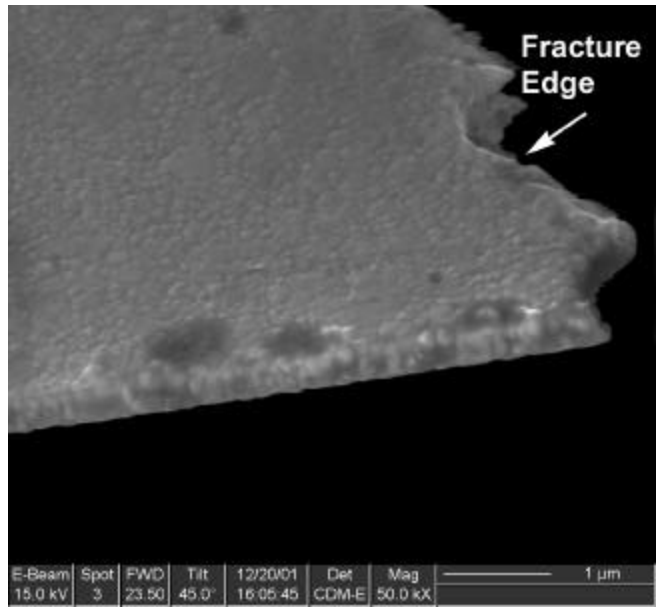

Fig. 7. SEM image of a fracture for a film thickness of 0.5 µm. Note the absence of deformation bands and zig-zag fracture surface.

passivated membrane occurred at a much lower state of stress and strain than the unpassivated membrane. The significant dissimilarity of residual and yield stresses of the two membranes show that the passivation layer had considerable effect on membrane uni-axial strength. Similar effects are seen in membranes of widths 2.5, 10, and 20.0 µm. Results of these tests are sumerized in Table 2. See Prorok and Espinosa [15] for stress-strain curves for these widths.

As membrane width was increased to 10 and 20 µm, residual stress leveled off to 29 MPa for the passivated membranes and 22 MPa for the unpassivated membranes. Yield stress for the passivated membranes increased slightly for the 10 µm specimen and decreased significantly for the 20 µm specimen. In the unpassivated membranes, yield stress decreased from 170 to 140 MPa with the increase in width.

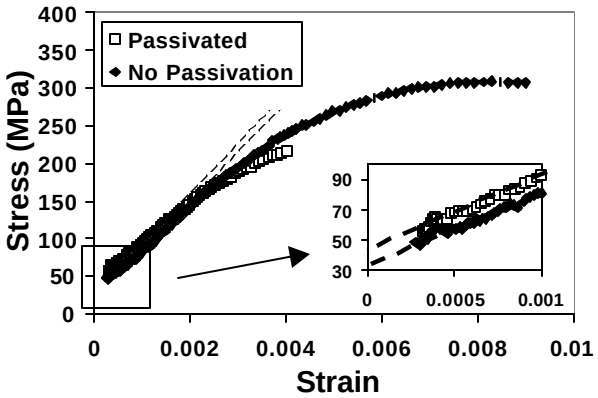

Fig. 8. Stress-Strain plots for membranes 5.0 µm wide comparing the effects of membranes with and without passivating layers.

These results clearly indicate that passivating the membranes significantly reduces their strength. This is in contrast to other studies that report an increase in strength [18-20]. However, in other experimental studies, the passivated film was studied in the presence of and confined by a rigid substrate and subject to large strain gradients during testing. The films were also only subjected to localized strains and stresses. The nature of the MDE test is such that the films are subjected to direct tensile testing with limited confinement and proportionally larger volumes of material subjected to uniform stresses. Thus, if a crack forms in the passivation layer, it may act as a stress concentrator and cause the Au membrane to fail at lower than normal stress and strain levels. This scenario is apparent in the SEM fracture image shown in Fig. 9. Clearly visible on both sides of the membrane are the fracture edges of the SiO_2 passivation layer. They are highlighted with arrows in the figure. Note that they run directly perpendicular to the membrane's width. Large plastic deformation of the gold seems to have been confined to this region where the passivation layer failed.

CONCLUSIONS

Young's modulus was consistently measured at 53-55 GPa for all specimens. Results indicated very strong effects of width and thickness on the films inelastic behavior. Although both dimensional parameters exhibited size effects, thickness, by far, had the greatest effect with a major transition in deformation behavior occurring when thickness was decreased from 1.0 to 0.5 µm, attributed to a reduction in the degrees of freedom for plastic deformation to occur due to the small number of grains through the thickness of the thinner specimens.

Results indicate that passivating the membrane's surfaces resulted in yield stress lower than unpassivated films of identical side for all membrane widths. Lower fracture strains

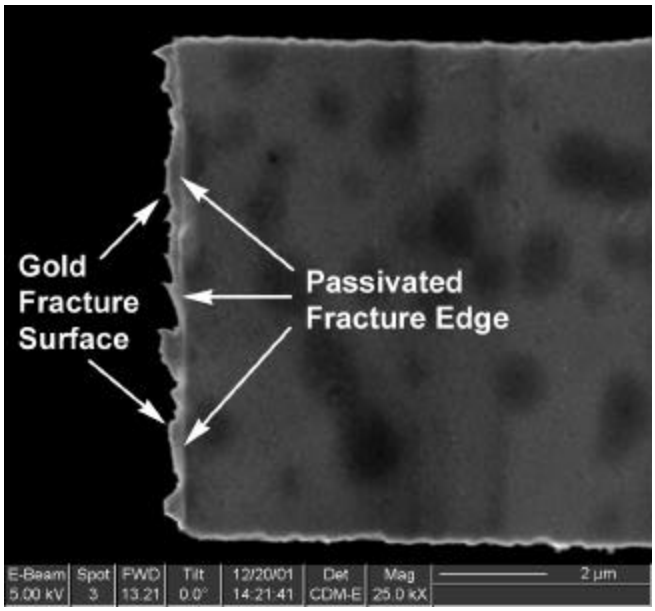

Fig. 9. SEM image of a fracture surface for the 2.5 µm wide passivated membrane.

and stresses and significantly larger states of residual stress were also found with passivation. Failure of the passivated membranes occurred where the passivating layer failed followed by localized plastic deformation of the gold confined to this region.

ACKNOWLEDGMENTS

This work was sponsored by the National Science Foundation under Career Award No. CMS-9624364 and the Office of Naval Research YIP through Award No. N00014-97-1-0550. Work was also supported in part by the Nanoscale Science and Engineering Initiative of the National Science Foundation under NSF Award Number EEC-0118025. Microscopy was carried out in the Center for Microanalysis of Materials, University of Illinois, which is partially supported by the U.S. Department of Energy under grant DEFG02-96-ER45439. Special thanks are due to G. Donahue and V. Diadiuk of the Microsystems Technology Lab at the Massachusetts Institute of Technology for their aid in microfabrication and W. Oliver and B. Peters of MTS Systems Corporation for their assistance in the utilization of the nanoindenter during this investigation.

REFERENCES

1. Q. Ma and D.R. Clark, Size dependent hardness of silver single crystals , J. of Mater. Res., Vol. 10, 853-863, 1995.
2. M. Atkinson, Further analysis of the size effect in indentation hardness tests of some metals, J. Mater. Res., Vol. 10, 2908-2915, 1995.
3. W.J. Poole, M.F. Ashby and N.A. Fleck, Micro-hardness of annealed and work-hardened copper polycrystals, Scripta Mater., Vol. 34, 599-564, 1996.
4. W.D. Nix, Elastic and plastic properties of thin films on substrates, Mater. Sci. Eng. A, Vol. 234-236, 37-44, 1997.
5. W.D. Nix and H. Gao, Indentation size effects in cryatalline materials: a law for strain gradient plasticity, J. Mech. Phys. Solids, Vol.46, 411-425, 1998.
6. N.A. Fleck, G.M. Muller, M.F. Ashby and J.W. Hutchinson, Strain gradient plasticity: theory and experiment, Acta Mater., Vol. 42, 475-487, 1994.
7. J.S. Stölken, and A.G. Evans, A microbend test method for measuring the plasticity length scale, Acta Mater., Vol. 46, 5109, 1998.
8. E.C. Aifantis, On the role of gradients in the locations of deformation and fracture, Int. J. Eng. Sci., Vol. 30, 1279-1299, 1992.
9. N.A. Fleck and J.W. Hutchinson, Strain gradient plasticity, Adv. Appl. Mech., Vol. 33, 295-361, 1997.
10. H. Gao, Y. Huang, W.D. Nix, and J.W. Hutchinson, Mechanism-based strain gradient plasticity-I. Theory, J. Mech. Phys. Solids, Vol. 47, 1239-1263, 1999.
11. J.W. Hutchinson, Plasticity at the micron scale, Int. J. Solids Struct., Vol. 37, 225-238, 2000.
12. H.D. Espinosa, B.C. Prorok, and M. Fischer, A novel experimental technique for testing thin films and MEMS materials, Proc. of the SEM Ann. Conf. on Exp. and Appl. Mech., June 4-6, 2001, Portland, Oregon, 446-449, 2001.
13. H.D. Espinosa, B.C. Prorok, and M. Fisher, Elasticity, plasticity, and fracture of thin films and MEMS materials – part I: a novel chip level testing methodology, submitted to J. Mech. Phys. Solids, 2001.
14. H.D. Espinosa and B.C. Prorok, Elasticity, plasticity, and fracture of thin films and MEMS materials – part II: size effects in submicron gold films, submitted to J. Mech. Phys. Solids, 2002.
15. B.C. Prorok and H.D. Espinosa, Effects of nanometer thick passivation layers on the mechanical response of thin gold films, submitted to J. Nanosci. Nanotech., 2001.
16. T.H. Courtney, in *Mechanical Behavior of Materials*, McGraw Hill, New York, 60, 1990.
17. K. Brown, Role of deformation and shear banding in the stability of the rolling textures of aluminum and an Al-0.8% Mg alloy, J. Inst. Met., Vol. 100, 341-345, 1972.
18. W.D. Nix, Mechanical properties of thin films, Met. Trans. A, Vol. 20A, 2217-2245, 1989.
19. S.C. Jain, A.H. Harker, and R.A. Cowley, Misfit strain and misfit dislocations in lattice mismatched Epitaxial layers and other systems, Phil. Mag. A, Vol. 75, 1461-1515, 1997.
20. M.J. Kobrinski and C.V. Thompson, The thickness dependence of the flow stress of capped and uncapped polycrystalline Ag thin films, Appl. Phys. Lett., Vol. 73, 2429- 2431, 1998.